

# CHAPTER

# 6

# Chapter 6. Modeling and IMC based PID Control of Single Input Single Output Unstable Nonlinear Process

---

## 6.1. Introduction

Continuous bioreactors find wide applications in wastewater treatment , fermentation processes, pharmaceutical industry, food industry, etc. (Bailey & Ollis, 1986). In recent years, various models for biochemical reactors have been developed to optimize the processes for the production of various products for agricultural, pharmaceuticals, sector etc. In industrial waste water treatment, membrane bioreactor technology is widely used. With this wide usage of bioreactor, there is a need to optimize and improve the bioreactor efficiency exercising proper control. Control of biochemical processes presents a challenge due to their nonlinear unstable multiple steady-state and hysteresis behaviour. Several relations have been developed between the substrate concentration and the growth rate coefficient in order to develop a dynamic model for the control of biochemical reactors in which the Monod and Substrate Inhibition Kinetic models are very common. In case of the Substrate Inhibition, numbers of steady state solutions are three in which two are stable but the conditions required for their use are not optimum. The third steady state is unstable but provides optimum operating conditions. Hence there is need for designing an efficient control system for the stabilized operation of a bioreactor (Simon, 2013).

One of the most critical process equipment from the control point of view that is widely used in the chemical and biochemical process industry is the Continuous Stirred Tank Reactor (CSTR) (Rao & Chidambaram, 2006). It is well established that the CSTR possesses nonlinear dynamic behaviour and also exhibits multiple steady states with the

possibility of one of the steady states being an unstable operating point (Bakošová et al., 2009; Pinheiro & Kershenbaum, 1999). The operation of CSTR at the high temperature (stable) steady state may be desirable in terms of higher conversion but the equipment design and plant safety issues associated with high temperature operation makes it unsafe. The best overall system performance is obtained at the intermediate temperature (unstable) steady-state point (Biagiola & Figueroa, 2004; Pinheiro & Kershenbaum, 1999). IMC based PID control of the CSTR at the unstable steady-state operating point is therefore studied.

## 6.2 Continuous Bioreactor

The schematic of a continuous stirred bioreactor is shown in Figure 6.1. The contents of the bioreactor are mixed thoroughly, ensuring uniform concentrations. The substrate is taken as input for the process which acts as a food for growth of biomass and its propagation. Substrate is quite often (but not necessarily) the pollutant/waste that gets consumed. Biomass is the biological cells that consume the substrate. The Monod Model and the Substrate Inhibition kinetic models have been used for present simulation.

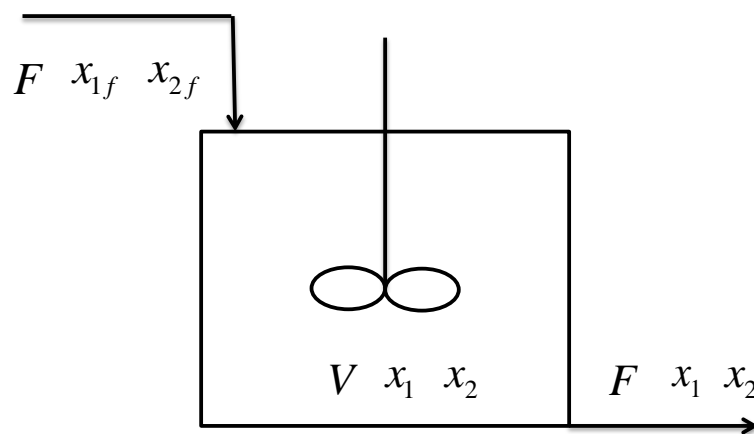


**Figure 6. 1 Schematic of Continuous Bioreactor**

### 6.2.1 Mathematical Modeling of the Continuous Bioreactor

The different process variables and system parameters involved in the development of mathematical model of a continuous well mixed bioreactor are shown in Table 6.1.

**Table 6. 1 Parameters and Variables in Continuous Bioreactor**

Variable/Parameter	Notation	Description
Biomass concentration	$x_1$	Mass of biomass cells/Volume
Biomass concentration in feed	$x_{1f}$	Mass of biomass cells/Volume
Substrate concentration	$x_2$	Mass of substrate/Volume
Substrate concentration in feed	$x_{2f}$	Mass of substrate/Volume
Rate of cell generation	$r_1$	Mass of biomass cells generated / (Volume)(time)
Volumetric flowrate	$F$	Volume/time
Specific growth rate coefficient	$\mu(x_2)$	Analogous to reaction rate constant
Rate of substrate consumption	$r_2$	Mass of substrate consumed/ (Volume)(time)
Yield	$Y$	Mass of biomass cells generated/Mass of substrate consumed
Bioreactor volume	$V$	
Dilution rate	$D$	Analogous to space velocity

#### 6.2.1.1 Unsteady State Mass Balances

Biomass material balance: Applying mass balance across the bioreactor for biomass gives:

$$\frac{dVx_1}{dt} = Fx_{1f} - Fx_1 + Vr_1 \quad \text{Eq. 6. 1}$$

Similarly, the material balance for the substrate gives:

$$\frac{dVx_2}{dt} = Fx_{2f} - Fx_2 - Vr_2 \quad \text{Eq. 6. 2}$$

The rate equation is given as:

$$r_1 = \mu x_1 \quad \text{Eq. 6. 3}$$

The yield is defined as:

$$Y = \frac{r_1}{r_2} \quad \text{Eq. 6. 4}$$

Equation 6.4 is written as:

$$r_2 = \frac{r_1}{Y} = \frac{\mu x_1}{Y} \quad \text{Eq. 6. 5}$$

Assuming the volume of reactor to be constant, the dilution rate is defined as:

$$D = \frac{F}{V} \quad \text{Eq. 6. 6}$$

The equations 6.1 and 6.2 are simplified as:

$$\frac{dx_1}{dt} = Dx_{1f} - Dx_1 + \mu x_1 \quad \text{Eq. 6. 7}$$

$$\frac{dx_2}{dt} = Dx_{2f} - Dx_2 - \frac{\mu x_1}{Y} \quad \text{Eq. 6. 8}$$

Assuming no biomass in feed:

$$x_{1f} = 0 \quad \text{Eq. 6. 9}$$

Equations 6.6 and 6.7 are simplified as:

$$f_1(x_1, x_2) = \frac{dx_1}{dt} = (\mu - D)x_1 \quad \text{Eq. 6. 10}$$

$$f_2(x_1, x_2) = \frac{dx_2}{dt} = D(x_{2f} - x_2) - \frac{\mu x_1}{Y} \quad \text{Eq. 6. 11}$$

Equations 6.9 and 6.10 represent the mathematical model of the continuous bioreactor in terms of two nonlinear functions,  $f_1$  and  $f_2$ .

### 6.2.1.2 Rate Equations

#### Monod Model:

The Monod model is analogous to the Langmuir adsorption isotherm. The Monod model is represented as:

$$\mu(x_2) = \frac{\mu_{\max} x_2}{k_m + x_2} \quad \text{Eq. 6. 12}$$

#### Substrate Inhibition (SI) Model:

In the Substrate Inhibition (SI) model, the toxicity of substrate is also considered. It is represented as:

$$\mu(x_2) = \frac{\mu_{\max} x_2}{k_m + x_2 + k_1 x_2^2} \quad \text{Eq. 6. 13}$$

In the Substrate Inhibition (SI) model, the growth rate coefficient ( $\mu$ ) reaches a maximum and then decreases at high substrate concentration ( $x_2$ ), due to the toxic effect on biomass cells. A comparison of the Monod model and the Substrate Inhibition (SI) model is shown in Figure 6.2.

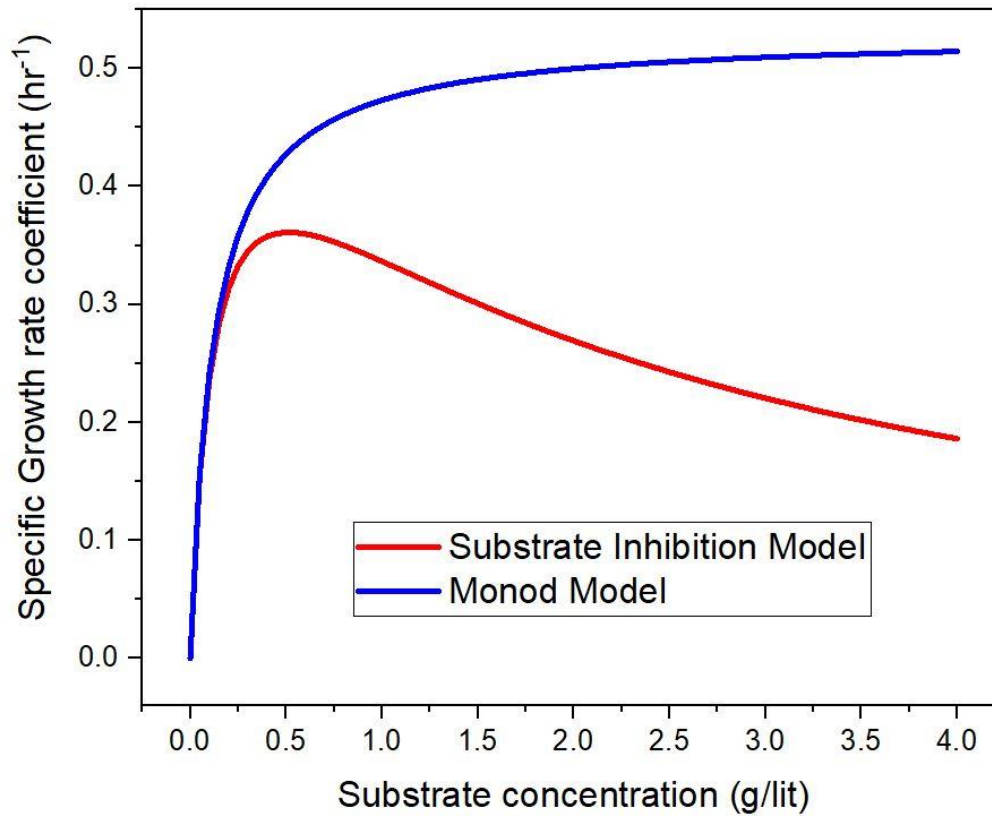


**Figure 6. 2 Comparison of the Monod and the Substrate Inhibition (SI) Models**

### 6.2.1.3 Steady State Solution of the Continuous Bioreactor

Parameters of the Substrate Inhibition (SI) model and the Monod model are shown in Table 6.2 and the operating conditions of the continuous bioreactor are shown in Table 6.3, (Agrawal & Lim, 1984), (Bequette, 1998).

**Table 6. 2 Parameters of the Substrate Inhibition Model and the Monod Model**

Model Parameter/Operating condition	Substrate Inhibition (SI) Model	Monod Model
$\mu_{\max}$ (hr <sup>-1</sup> )	0.53	0.53
$k_m$ (g/lit)	0.12	0.12
$k_1$ (lit/g)	0.4545	NA

**Table 6. 3 Operating conditions of the Continuous Bioreactor**

Operating Variable	Value
Substrate concentration in feed, $x_{2f}$ (g/lit)	4.0
Biomass concentration in feed, $x_{1f}$ (g/lit)	0
Dilution rate, $D$ (hr <sup>-1</sup> )	0.30

The steady state solution is obtained by setting the derivative terms of equations 6.9 and 6.10 to zero. The subscript ‘s’ is used to denote the steady state condition. The steady state equations are given as:

$$\frac{dx_{1s}}{dt} = (\mu_s - D_s)x_{1s} = 0 \quad \text{Eq. 6. 14}$$

$$\frac{dx_{2s}}{dt} = D_s(x_{2fs} - x_{2s}) - \frac{\mu_s x_{1s}}{Y} = 0 \quad \text{Eq. 6. 15}$$

The above steady state equations have two solutions:

1. Steady state solution 1: It is also called the trivial solution (Washout condition). It represents no conversion as all the biomass cells are washed out of the bioreactor.

The trivial solution of equations 6.13 and 6.14 is given as:

$$x_{1s} = 0 \quad \text{Eq. 6. 16}$$

$$x_{2s} = x_{2fs} \quad \text{Eq. 6. 17}$$

2. Steady state solution 2: The non-trivial solution ( $x_{1s} \neq 0$ ) of equations 6.13 and 6.14 is given as:



$$\mu_s(x_{2s}) = D_s \quad \text{Eq. 6. 18}$$

$$x_{1s} = Y(x_{2fs} - x_{2s}) \quad \text{Eq. 6. 19}$$

The solution of  $x_{2s}$  is obtained by substituting equation 6.17 into the Substrate Inhibition (SI) model (equation 6.12). The Substrate Inhibition (SI) model equation is quadratic and has two solutions, which are represented as:

$$x_{2s} = \frac{-\left[1 - \frac{\mu_{\max}}{D_s}\right] \pm \sqrt{\left[1 - \frac{\mu_{\max}}{D_s}\right]^2 - 4k_1k_m}}{2k_1} \quad \text{Eq. 6. 20}$$

#### 6.2.1.4 Linearized State Space Model of the Continuous Bioreactor

The linearized state space model of the continuous bioreactor is obtained from the nonlinear model equations (equations 6.10 and 6.11).

The (2x1) vector of state variables (in deviation form) is defined as:

$$\mathbf{x} = [x_1, x_2]^T = [(x_1 - x_{1s}), (x_2 - x_{2s})]^T \quad \text{Eq. 6. 21}$$

The (2x1) vector of time derivatives of state variables (in deviation form) is defined as:

$$\dot{\mathbf{x}} = [dx_1 / dt, dx_2 / dt]^T \quad \text{Eq. 6. 22}$$

The (2x1) vector of input variables (in deviation form) is defined as:

$$\mathbf{u} = [u_1, u_2]^T = [(D - D_s), (x_{2f} - x_{2fs})]^T \quad \text{Eq. 6. 23}$$

The elements of (2x2)  $\mathbf{A}$  matrix of the state space model (equation 3. 96) are given as:

$$a_{11} = \mu_s - D_s \quad \text{Eq. 6. 24}$$

$$a_{12} = x_{1s} \mu_s' \quad \text{Eq. 6. 25}$$

Where,  $\mu'_s$  is defined as:

$$\mu'_s = \frac{\partial \mu_s}{\partial x_{2s}} = \frac{\mu_{\max} (k_m - k_1 x_{2s}^2)}{(k_m + x_{2s} + k_1 x_{2s}^2)^2} \quad \text{Eq. 6. 26}$$

$$a_{21} = -\frac{\mu_s}{Y} \quad \text{Eq. 6. 27}$$

$$a_{22} = -D_s - \frac{\mu'_s x_{1s}}{Y} \quad \text{Eq. 6. 28}$$

Similarly, the elements of (2x2) **B** matrix of the state space model (equation 3. 96) are given as:

$$b_{11} = -x_{1s} \quad \text{Eq. 6. 29}$$

$$b_{12} = 0 \quad \text{Eq. 6. 30}$$

$$b_{21} = x_{2fs} - x_{2s} \quad \text{Eq. 6. 31}$$

$$b_{22} = D_s \quad \text{Eq. 6. 32}$$

### 6.2.1.5 Stability Analysis of the Continuous Bioreactor

The stability analysis is carried out by calculating the Eigen values of the **A** matrix (equations 6.24-6.28). The two Eigen values ( $\alpha_1$  and  $\alpha_2$ ) are given as :

$$\alpha_1 = -D_s \quad \text{Eq. 6. 33}$$

$$\alpha_2 = -\frac{\mu'_s x_{1s}}{Y} - \mu_s + D_s \quad \text{Eq. 6. 34}$$

Since the dilution rate,  $D_s$  is always positive, equation 6.33 shows:

$$\alpha_1 < 0 \quad \text{Eq. 6. 35}$$

One of the Eigen values,  $\alpha_1$  is always negative.

Stability of the non-trivial solution:

For the non-trivial solution (equations 6.18 and 6.19),

$$\alpha_2 = -\frac{\mu'_s x_{1s}}{Y} \quad \text{Eq. 6. 36}$$

The Eigen value  $\alpha_2$  may be negative or positive depending on the sign of the slope of the growth rate coefficient ,  $\mu'_s$ . Accordingly, the following two cases are possible:

$$\text{Case A: If } \mu'_s > 0, \text{ then } \alpha_2 < 0 \quad \text{Eq. 6. 37}$$

In this case, since both the Eigen values are negative, hence, the system is stable.

$$\text{Case B: If } \mu'_s < 0, \text{ then } \alpha_2 > 0 \quad \text{Eq. 6. 38}$$

In this case, since one of the Eigen values,  $\alpha_2$  is positive, hence, the system is unstable.

Stability of the trivial solution:

For the trivial solution (equations 6.16 and 6.17), the stability condition is given as:

$$D_s > \mu_s \quad \text{Eq. 6. 39}$$

Based on the Substrate Inhibition (SI) model, the three steady state solutions (one trivial solution and two nontrivial solutions) corresponding to the input operating conditions (Table 6.3) of the continuous bioreactor, are shown in Table 6.4. One of the two non-trivial solutions is unstable.

**Table 6. 4 Stability analysis of steady states in continuous bioreactor**

Kinetic Model	Substrate Inhibition Model		
	Trivial Solution	Non trivial Solution 1	Non trivial Solution 2
$x_{1s}$	0	0.9951	1.5302
$x_{2s}$	4.0	1.5123	0.1746
$\mu_s$	0.1861	0.3	0.3
$\mu'_s$	-0.0292	-0.0683	0.5913
$\alpha_1$	-0.3	-0.3	-0.3
$\alpha_2$	-0.1139	+0.1698	-2.2619
Remark	Stable ( $D_s > \mu_s$ )	Unstable ( $\mu'_s < 0$ )	Stable

### 6.2.1.6 Degrees of Freedom Analysis of the Continuous Bioreactor

The degrees of freedom analysis is useful in identifying the number of state variables to be measured (measured outputs) and the number of controllers required. In the case of continuous bioreactor, the total number of variables is  $n_v = 4$ , total number of equations is  $n_e = 2$  (equations 6.14 and 6.15). The degrees of freedom, is  $f = n_v - n_e = 2$ . One of the two input variables, (substrate concentration in feed,  $x_{2f}$ ) is specified. Therefore, the number of measured outputs and the number of controllers required is one. The control objective is to design a suitable controller to control the biomass concentration (controlled variable),  $x_1$  using the dilution rate,  $u_1$  as the manipulated variable.

### 6.2.1.7 Transfer Function Model of the Continuous Bioreactor

The transfer function model (equations 3.103 and 3.104) of the continuous bioreactor is obtained for the unstable steady state (non trivial solution 1). The transfer function of the biomass concentration with respect to the dilution rate is given as:

$$g_{11}(s) = \frac{x_1(s)}{u_1(s)} = \frac{5.8604}{-5.8893s + 1} \quad \text{Eq. 6. 40}$$

Similarly, the transfer function of the substrate concentration with respect to the dilution rate is given as:

$$g_{21}(s) = \frac{x_2(s)}{u_1(s)} = \frac{-14.6508}{-5.8893s + 1} \quad \text{Eq. 6. 41}$$

The pole of the transfer functions,  $g_{11}(s)$  and  $g_{21}(s)$  is obtained from the solution of the denominator polynomial (characteristic equation) as:

$$-5.8893s + 1 = 0 \quad \text{Eq. 6. 42}$$

$$p = +0.1698 \quad \text{Eq. 6. 43}$$

The pole of the transfer functions,  $g_{11}(s)$  and  $g_{21}(s)$  is same as the Eigen value,  $\alpha_2$  (Table 6.4). Since the location of the pole of the transfer functions,  $g_{11}(s)$  and  $g_{21}(s)$  is on the Right Half Plane (RHP), the transfer functions,  $g_{11}(s)$  and  $g_{21}(s)$  represent first order unstable processes.

### 6.2.2 IMC based PI Controller Design for the Continuous Bioreactor

The process transfer function of bioreactor is unstable first order as shown in equation 6.40. To control the open loop unstable process, an Internal Model Control (IMC) based Proportional Integral (PI) controller is designed based on equations 3.60 and 3.61 (section

3.2.4) . The Integral of Square of Error (ISE) is used as the Quantitative Performance Index (QPI) to select the optimum value of the Internal Model Control (IMC) based PI controller tuning parameter,  $\lambda$ , as shown in Figure 6.3.

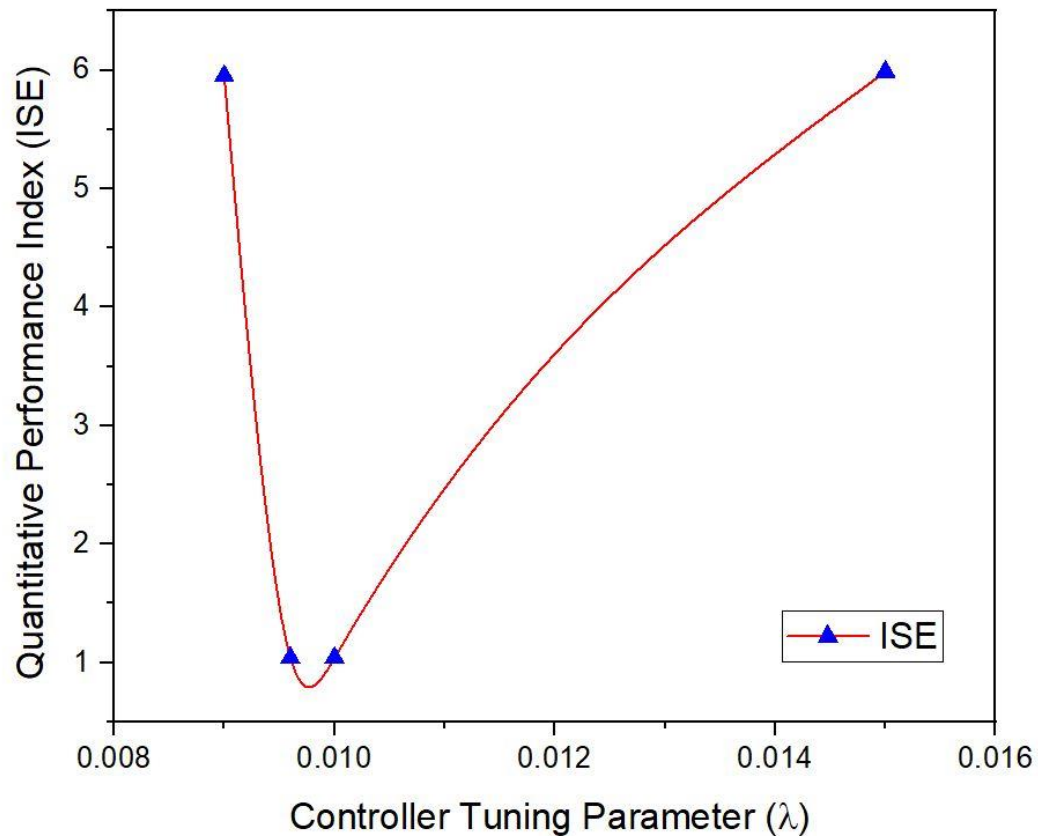


**Figure 6. 3 Tuning of IMC based PI Controller for Continuous Bioreactor**

### **6.2.3 Closed loop Response of the IMC based PI Controller**

The closed loop response of the Internal Model Control (IMC) based Proportional Integral (PI) controller, to step change in the biomass concentration (servo problem) is shown in Figure 6.4. The designed controller has good set point tracking properties (minimum overshoot and zero offset).

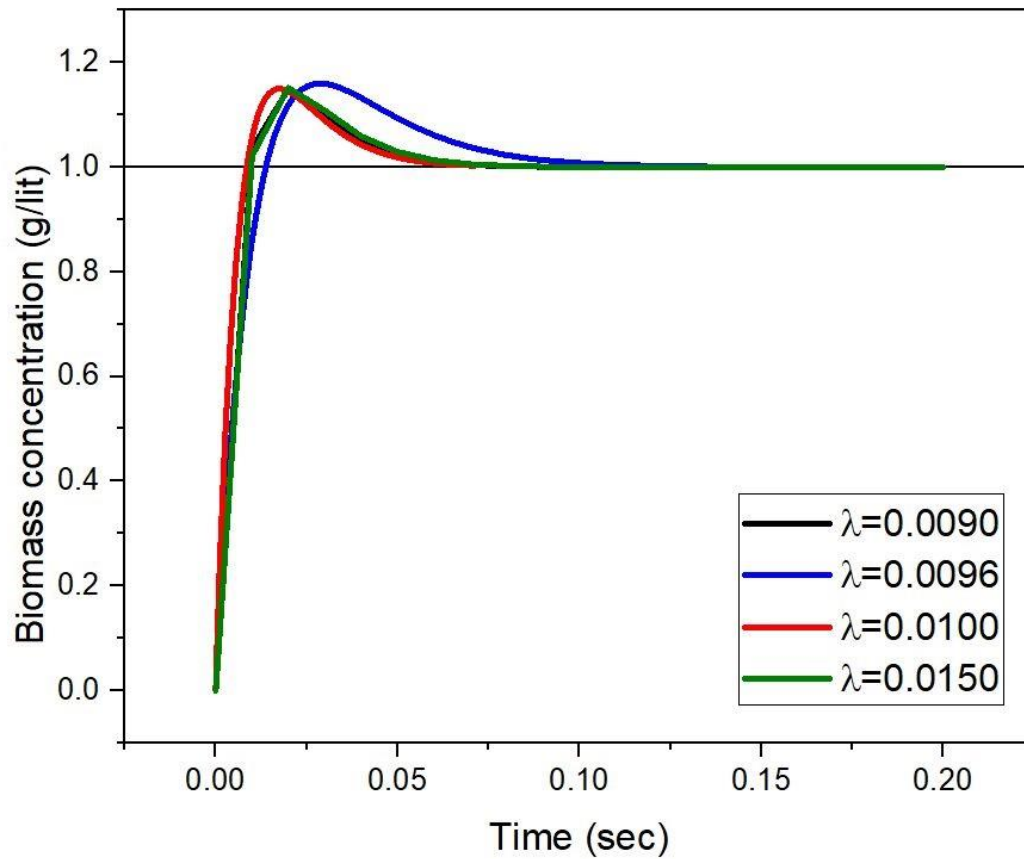


**Figure 6. 4 Closed loop response of Bioreactor with IMC based PID controller**

#### **6.2.4 Conclusion**

The mathematical model of a continuous bioreactor based on substrate inhibition kinetic model is developed. The continuous bioreactor has multiple steady-states. From the stability analysis, it is observed that one of the three steady states is unstable. An Internal Model Control (IMC) based PI controller is designed to control the biomass concentration in the continuous bioreactor. Efficient control of the continuous bioreactor at the unstable steady state operating point is achieved by optimum tuning of the controller parameter.

### 6.3 Non-Adiabatic Jacketed CSTR

Consider a constant volume non-adiabatic jacketed Continuous Stirred Tank Reactor (CSTR) (Bequette, 2003), as shown in Figure 6.5. A first order exothermic reaction  $A \xrightarrow{k} B$  takes place within the reactor.

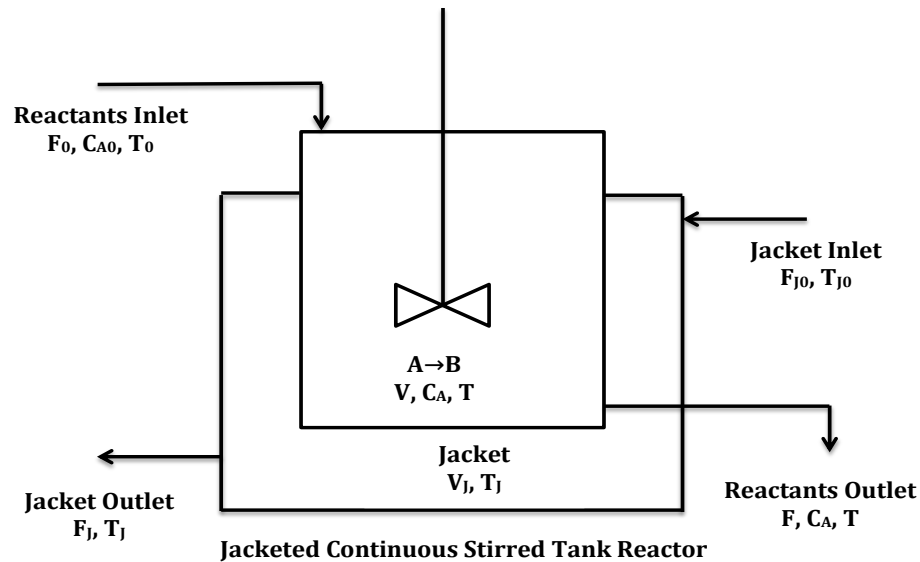


Figure 6. 5 Schematic of the Non-adiabatic Jacketed CSTR

#### 6.3.1 Mathematical Model of the Non-adiabatic Jacketed CSTR

The contents of the non-adiabatic jacketed Continuous Stirred Tank Reactor (CSTR) are assumed to be perfectly mixed. The model equations of the CSTR and jacket are obtained by writing the mass and energy balances:

##### 6.3.1.1. Unsteady State Mass and Energy Balances

The total mass balance equation for the reactor is written as:

$$\frac{d}{dt}(\rho V) = F_i \rho_i - F \rho \quad \text{Eq. 6. 44}$$

Assuming constant density and constant volume of the reactor, equation 6.44 is simplified as:



$$F_i = F \quad \text{Eq. 6. 45}$$

The component mass balance equation for the reactor is written as:

$$f_1(C_A, T) = \frac{dC_A}{dt} = \frac{F}{V}(C_{A0} - C_A) + r_A \quad \text{Eq. 6. 46}$$

The energy balance equation for the reactor is written as:

$$f_2(C_A, T) = \frac{dT}{dt} = \frac{F}{V}(T_0 - T) + \frac{\Delta H}{\rho c_p} r_A - \frac{UA_H}{V \rho C_p}(T - T_J) \quad \text{Eq. 6. 47}$$

The reaction kinetics is expressed as:

$$r_A = -kC_A = -k_0 \exp(-\Delta E / RT)C_A \quad \text{Eq. 6. 48}$$

### 6.3.1.2 Steady State Solution of the Non-adiabatic Jacketed CSTR

The input operating conditions and the design parameters of the non-adiabatic jacketed CSTR are shown in Table 6.5.

**Table 6. 5 Operating Conditions and Design Parameters of the CSTR**

Process Parameters	Input variables	Value
$F/V$ (hr <sup>-1</sup> )		1
$k_0$ (hr <sup>-1</sup> )		9703*3600
$\Delta H$ (Kcal/kmol)		-5960
$\Delta E$ (Kcal/kmol)		11843
$\rho C_p$ (Kcal/ m <sup>3</sup> °C)		500
$UA_H / V$ (Kcal/m <sup>3</sup> °C hr)		150
$T_J$ (K)		298
	$T_0$ (K)	298
	$C_{A0}$ (Kmol/m <sup>3</sup> )	10

The steady state solution is obtained from the solution of the mathematical model (equations 6.48 and 6.49) based on the input operating conditions and the design parameters (Table 6.5). Under steady state conditions, the time derivatives in the differential equations (equations 6.48 and 6.49) vanish resulting in two nonlinear algebraic equations (in two unknowns,  $C_A$  and  $T$ ), whose solution is numerically obtained by the multivariable Newton Raphson method (Appendix A).

The non-adiabatic jacketed CSTR has three steady state solutions: (1) the low temperature, low conversion steady state, (2) the intermediate temperature, intermediate conversion steady state, and (3) the high temperature, high conversion steady state, as shown in Table 6.6.

**Table 6. 6 Multiple Steady States in the Non-adiabatic Jacketed CSTR**

<b>Steady state solution</b>	<b>Low temperature, low conversion steady state</b>	<b>Intermediate temperature, Intermediate conversion steady state</b>	<b>High temperature, high conversion steady state</b>
$C_{As}$ (Kmol/m <sup>3</sup> )	8.56	5.52	2.36
$T_s$ (K)	311.2	339.1	368.1

### 6.3.1.3 Linearized State Space Model of the Non-adiabatic Jacketed CSTR

The linearized state space model of the non-adiabatic jacketed CSTR is obtained from the nonlinear model equations (equations 6.46 and 6.47) .

The (2x1) vector of state variables (in deviation form) is defined as:

$$\mathbf{x} = [x_1, x_2]^T = [(C_A - C_{As}), (T - T_s)]^T \quad \text{Eq. 6. 49}$$

The (2x1) vector of time derivatives of state variables (in deviation form) is defined as:

$$\dot{\mathbf{x}} = [\dot{x}_1, \dot{x}_2]^T = [(dC_A / dt), (dT / dt)]^T \quad \text{Eq. 6. 50}$$

The (3x1) vector of input variables (in deviation form) is defined as:

$$\mathbf{u} = [u_1, u_2, u_3]^T = [(T_J - T_{Js}), (C_{A0} - C_{A0s}), (T_0 - T_{0s})]^T \quad \text{Eq. 6. 51}$$

The elements of (2x2) **A** matrix of the state space model (equation 3. 96) are given as:

$$a_{11} = -(F / V) - k_s \quad \text{Eq. 6. 52}$$

$$k'_s = \left( \frac{\partial k}{\partial T} \right) \Big|_s = k_s \left( \frac{\Delta E}{RT_s^2} \right) \quad \text{Eq. 6. 53}$$

$$a_{12} = -C_{As} k'_s \quad \text{Eq. 6. 54}$$

$$a_{21} = -(\Delta H / \rho C_p) k_s \quad \text{Eq. 6. 55}$$

$$a_{22} = -(F / V) - \frac{UA_H}{V \rho C_p} - \frac{\Delta H}{\rho C_p} C_{As} k'_s \quad \text{Eq. 6. 56}$$

Similarly, the elements of (2x3) **B** matrix of the state space model (equation 3. 96) are given as:

$$b_{11} = 0 \quad \text{Eq. 6. 57}$$

$$b_{12} = (F / V) \quad \text{Eq. 6. 58}$$

$$b_{13} = 0 \quad \text{Eq. 6. 59}$$

$$b_{21} = \frac{UA_H}{V \rho C_p} \quad \text{Eq. 6. 60}$$

$$b_{22} = 0 \quad \text{Eq. 6. 61}$$

$$b_{23} = (F/V) \quad \text{Eq. 6. 62}$$

#### 6.3.1.4 Stability Analysis of the Non-adiabatic Jacketed CSTR

The stability analysis is carried out by calculating the Eigen values of the **A** matrix of the state space model (equations 6.52-6.56). Corresponding to each of the three steady states (Table 6.6) of the non-adiabatic jacketed CSTR, the Eigen values ( $\alpha_1$  and  $\alpha_2$ ) are calculated, as shown in Table 6.7.

**Table 6. 7 Steady State Multiplicity and Stability Analysis of the CSTR**

Steady state	Eigen value, $\alpha_1$	Eigen value, $\alpha_2$	Stability Analysis
Low temperature, low conversion steady state	-0.90	-0.52	Open loop Stable (the two Eigen values are real and negative)
Intermediate temperature, Intermediate conversion steady state	-0.84	+0.50	Open loop Unstable (One Eigen value is positive)
High temperature, high conversion steady state	$-0.77 + 0.96 i$	$-0.77 - 0.96 i$	Open loop Stable (The two Eigen values are complex conjugates with negative real part)

Based on the Eigen values, ( $\alpha_1$  and  $\alpha_2$ ), the following inferences are drawn with regard to stability of each of the three steady states:

- a. Stability of Low temperature, low conversion steady state:

Since the two Eigen values are real and negative, the low temperature, low conversion steady state is open loop stable.

b. Stability of intermediate temperature, intermediate conversion steady state:

Since one of the Eigen values is positive, the intermediate temperature, intermediate conversion steady state is open loop unstable. (Anusha & Rao, 2012).

c. Stability of high temperature, high conversion steady state:

Since the two Eigen values are complex conjugates with negative real part, the high temperature, high conversion steady state is also open loop stable.

### 6.3.1.6 Degrees of Freedom Analysis

The classification of process outputs (state variables or controlled variables), process inputs (disturbance and manipulated variables) and the process parameters are shown in Table 6.8.

**Table 6. 8 Classification of variables and parameters in the Non-adiabatic Jacketed CSTR**

State variables		Process Input variables		Process Parameters
Unmeasured	Measured Controlled variables (CV)	Manipulated Variables (MV)	Disturbance Variables (DV)	
$C_A$	$T$	$T_J$	$C_{A0}$ $T_0$	$k_0, \Delta E, \Delta H,$ $UA, V, F,$ $\rho C_p$

The degrees of freedom analysis helps in (a) deciding the number of control loops required, and (b) deciding the proper pairing of the controlled variables (CV) with the Manipulated Variables (MV).

For the case of the Non-adiabatic Jacketed CSTR, the number of independent equations  $n_e = 2$  and the number of variables  $n_v = 5$ . The degrees of freedom is  $f = 3$ . In order to obtain a unique solution, the degrees of freedom must be reduced to zero. This is accomplished by:

- a) specifying the values of two disturbance variables (DV),  $C_{A0}$  and  $T_0$ , and,
- b) Writing one controller equation relating the controlled variables (CV),  $T$  with the Manipulated Variables (MV),  $T_j$ .

Based on the degrees of freedom analysis, the reactor temperature is selected as the controlled variable (CV), since the online and continuous measurement of temperature is easier than the measurement of concentration. The degrees of freedom analysis also suggests that the reactor concentration gets automatically controlled by controlling the reactor temperature and that no additional control loop for the control of reactor concentration is necessary.

### **6.3.1.7 Transfer Function Model of the Non-adiabatic Jacketed CSTR**

The transfer function model (equations 3.103 and 3.104) of the non-adiabatic jacketed CSTR is obtained corresponding to the unstable intermediate temperature, intermediate conversion steady state.

The transfer function of the reactor concentration,  $C_A$  with respect to the jacket temperature,  $T_j$  is given as:

$$g_{11}(s) = \frac{x_1(s)}{u_1(s)} = \frac{-0.07}{s^2 + 0.34s - 0.42} \quad \text{Eq. 6. 63}$$

The transfer function,  $g_{11}(s)$  (equation 6.63) suggests that the reactor concentration,  $C_A$  follows second order dynamics with respect to change in the jacket temperature,  $T_j$ .

Similarly, the transfer function of the reactor temperature,  $T$  with respect to the jacket temperature,  $T_j$  is given as:

$$g_{21}(s) = \frac{0.3s + 0.54}{s^2 + 0.34s - 0.42} \quad \text{Eq. 6. 64}$$

The transfer function,  $g_{21}(s)$  (equation 6.64) suggests that the reactor temperature,  $T$  follows numerator dynamics (relative order of transfer function is first order) with respect to change in the jacket temperature,  $T_j$ .

The poles of the transfer functions,  $g_{11}(s)$  and  $g_{21}(s)$  are obtained from the solution of the denominator polynomial (characteristic equation) as shown:

$$(s^2 + 0.34s - 0.42) = 0 \quad \text{Eq. 6. 65}$$

The two poles are given as:

$$p_1 = -0.84 \quad \text{Eq. 6. 66}$$

$$p_2 = 0.5 \quad \text{Eq. 6. 67}$$

The two poles of the transfer functions,  $g_{11}(s)$  and  $g_{21}(s)$  are same as the two Eigen values, ( $\alpha_1$  and  $\alpha_2$ ) of the  $\mathbf{A}$  matrix of the state space model (equation 3. 96).

### 6.3.2 IMC based PID Controller Design for the Non-adiabatic Jacketed CSTR

In order to control the temperature of the non-adiabatic jacketed CSTR at its unstable steady state, an Internal Model Control (IMC) based PI controller cascaded with a lead lag filter is designed, based on equations 3.69 and 3.70 (section 3.2.5).

The Integral of Square of Error (ISE) is used as the Quantitative Performance Index (QPI) to select the optimum value of the controller tuning parameter,  $\lambda$ , as shown in Figure 6.6.

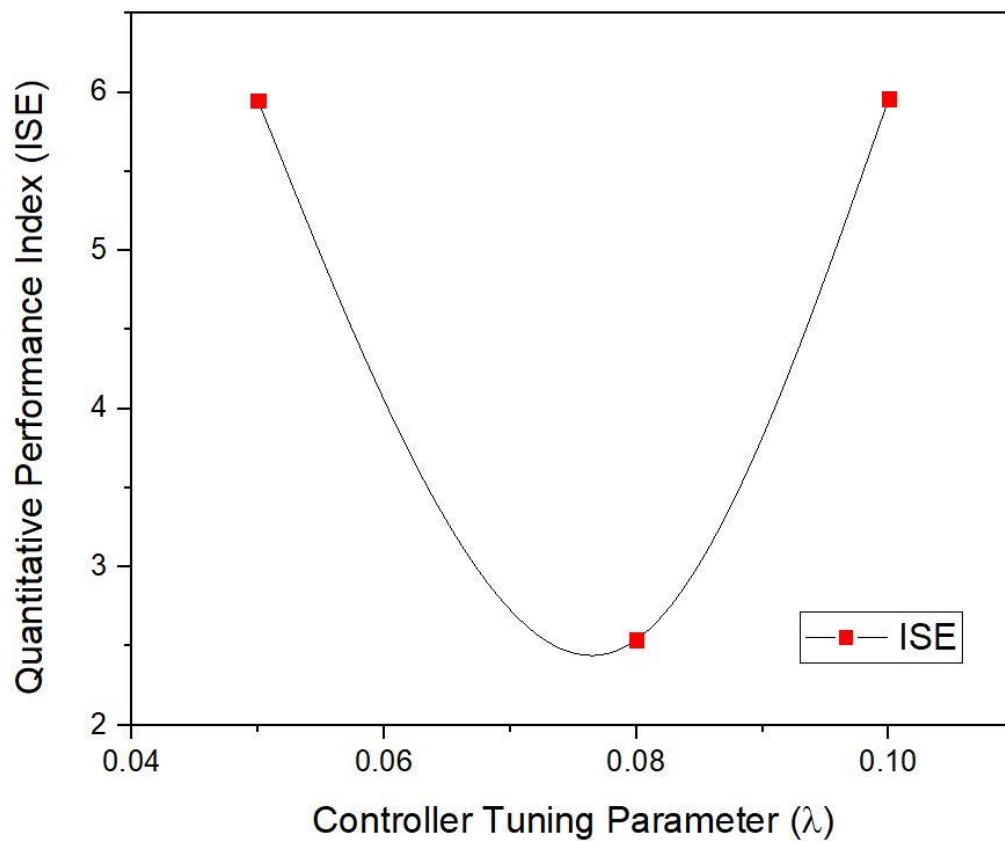


Figure 6. 6 IMC based PID controller tuning of the Non-adiabatic Jacketed CSTR



### 6.3.3 Closed loop Response of the IMC based PI Controller

For a step change in the reactor temperature set point (servo problem), the closed loop response of the Internal Model Control (IMC) based Proportional Integral (PI) controller is studied for different values of the controller tuning parameter,  $\lambda$ . The designed controller has good set point tracking properties (minimum overshoot and zero offset) as shown in Figure 6.7.

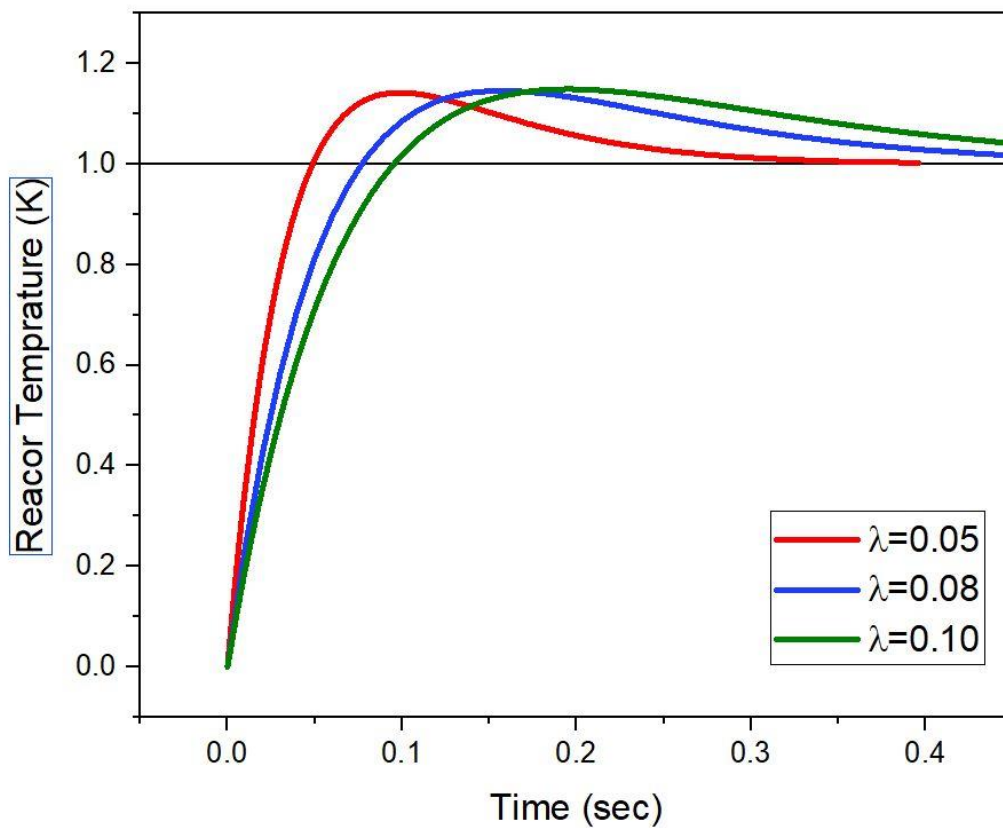


Figure 6. 7 Closed loop response of IMC based PID controller

### **6.3.4 Conclusion**

The conventional methods of PID based controller tuning may work well for open loop stable systems; but in case of open loop unstable systems (as exemplified by the non-adiabatic jacketed CSTR) the Internal Model Control (IMC) based PID tuning method proves to be superior. From the closed loop response of the system, it is observed that the dynamics of the system is fast enough to warrant a satisfactory operation of the non-adiabatic jacketed CSTR at the unstable steady state. The performance indices also show promising results for the tuning method used for this problem.